Supporting Material for

Glucosylceramide reorganizes cholesterol-containing domains in a fluid phospholipid membrane

Ana R.P. Varela,[1,2,3] André Sá Couto,[1] Aleksander Fedorov,[2] Anthony H. Futerman,[3] Manuel Prieto,[2] and Liana C. Silva[1],*

[1] iMed.ULisboa –Research Institute for Medicines, Faculdade de Farmácia, Universidade de Lisboa, Av. Professor Gama Pinto, 1649-003 Lisbon, Portugal
[2] Centro de Química-Física Molecular & IN - Institute of Nanoscience and Nanotechnology, Instituto Superior Técnico, Universidade de Lisboa, Lisboa, Av. Rovisco Pais, 1049-001 Lisbon, Portugal
[3] Department of Biological Chemistry, Weizmann Institute of Science, Rehovot 76100, Israel

*Corresponding author:

Liana C. Silva, Research Institute for Medicines (iMed.ULisboa), Faculdade de Farmácia, Universidade de Lisboa, Av. Professor Gama Pinto, 1649-003 Lisbon - Portugal Tel: + 351 217 946 400 (ext 14204), Fax: + 351 217 937 703, Email: lianacsilva@ff.ul.pt

Supplementary Figures

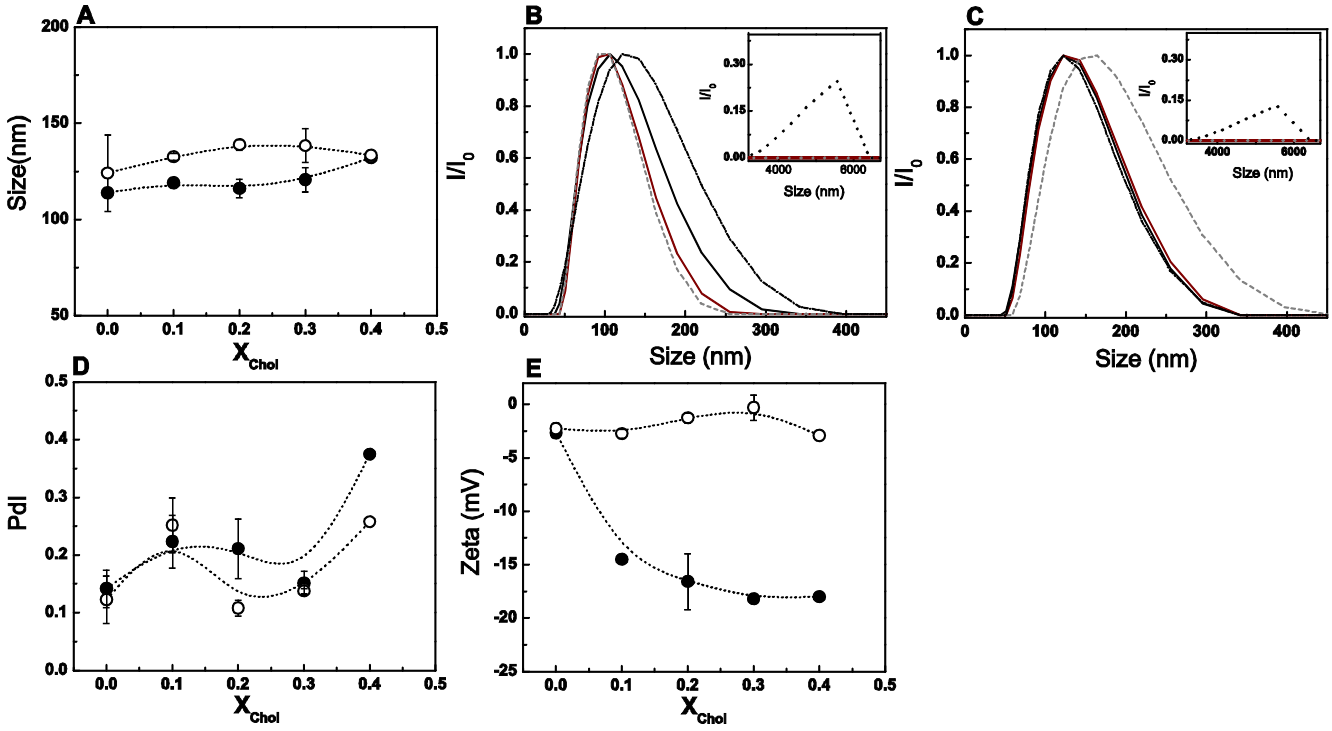

Figure S1. Characterization of POPC/Chol binary mixtures by electrophoretic and dynamic light scattering measurements.

(A) Average size of POPC/Chol LUVs at neutral (solid symbols) and acidic (open symbols) pH. (B, C) Normalized scattered light intensity of LUVs composed by POPC with 10 (—), 20 (—), 30 (---) and 40 (-.-.-) mol % of Chol at (B) pH 7.4 and (C) 5.5. Inset shows vesicle population with sizes in the order of microns. These liposomes represent a very small population of the sample. This was confirmed by the disappearance of the very high size band, when the number of the vesicles was considered instead of the scattering intensity (data not shown). (D) Polidispersity index (PdI) and (E) ζ-potential of POPC/Chol LUVs at neutral (solid symbols) and acidic (open symbols) pH. Values are means ± SD of at least 3 independent experiments.

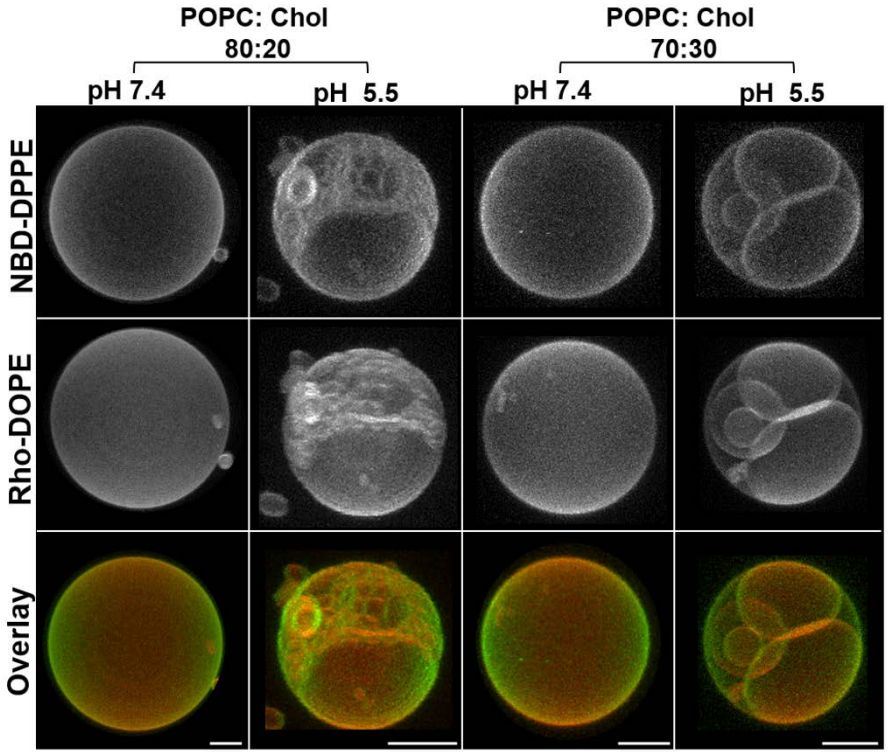

Figure S2. Confocal fluorescence microscopy of POPC/Chol mixtures.

3D projection images from confocal slices (0.4 µm) of POPC/Chol GUVs labelled with NBD-DPPE and Rho-DOPE at neutral and acidic pH. Scale bar, 5 µm

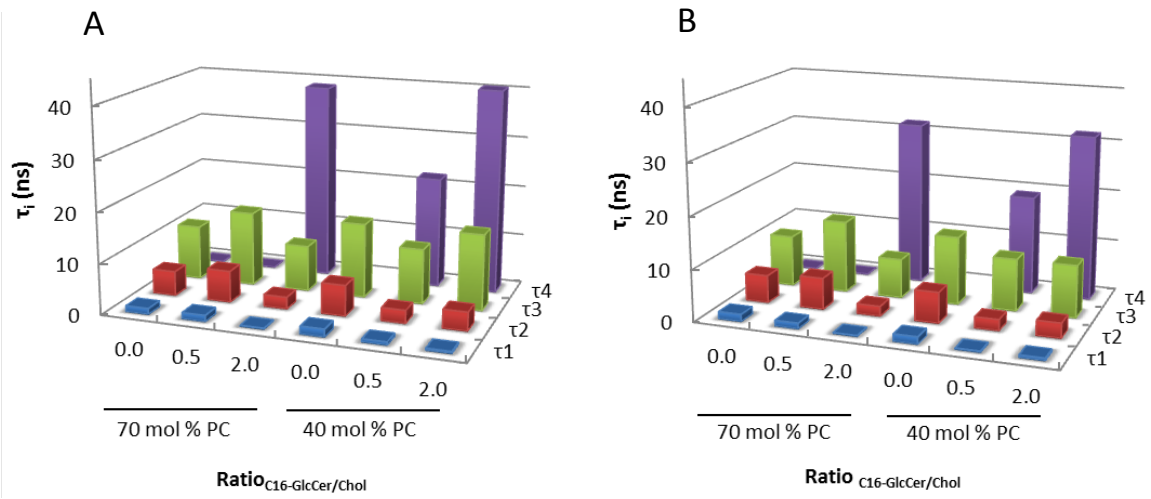

Figure S3. Lifetime components of t-PnA fluorescence intensity decay in mixtures of POPC/Chol/C16-GlcCer with different C16-GlcCer/Chol ratios.

Variation of the lifetime components of t-PnA fluorescence intensity decay in POPC/Chol/C16-GlcCer. The mixtures contain 40 and 70 mol % of POPC. Measurements were performed at (A) pH 7.4 and (B) pH 5.5.Values are means of at least 3 independent experiments.

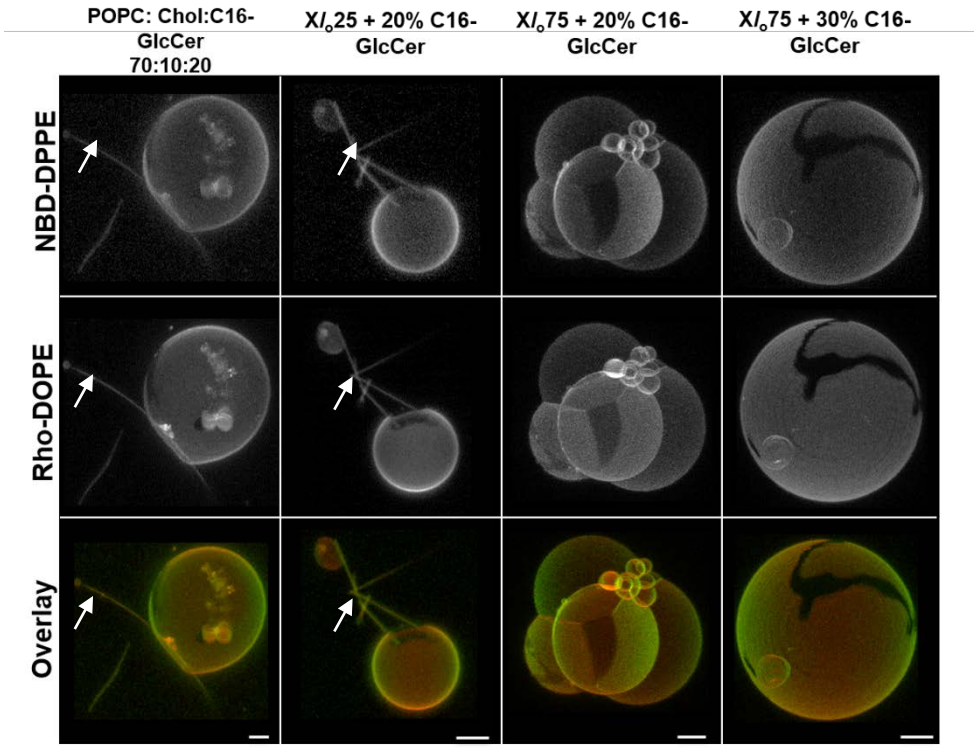

Figure S4. Morphological alterations of POPC/Chol/C16-GlcCer mixtures at acidic pH.

3D projection images from 0.4 µm confocal slices of POPC/Chol/C16-GlcCer GUVs labelled with NBD-DPPE and Rho-DOPE. Tubules are highlighted with white arrows. Scale bar, 5 µm.

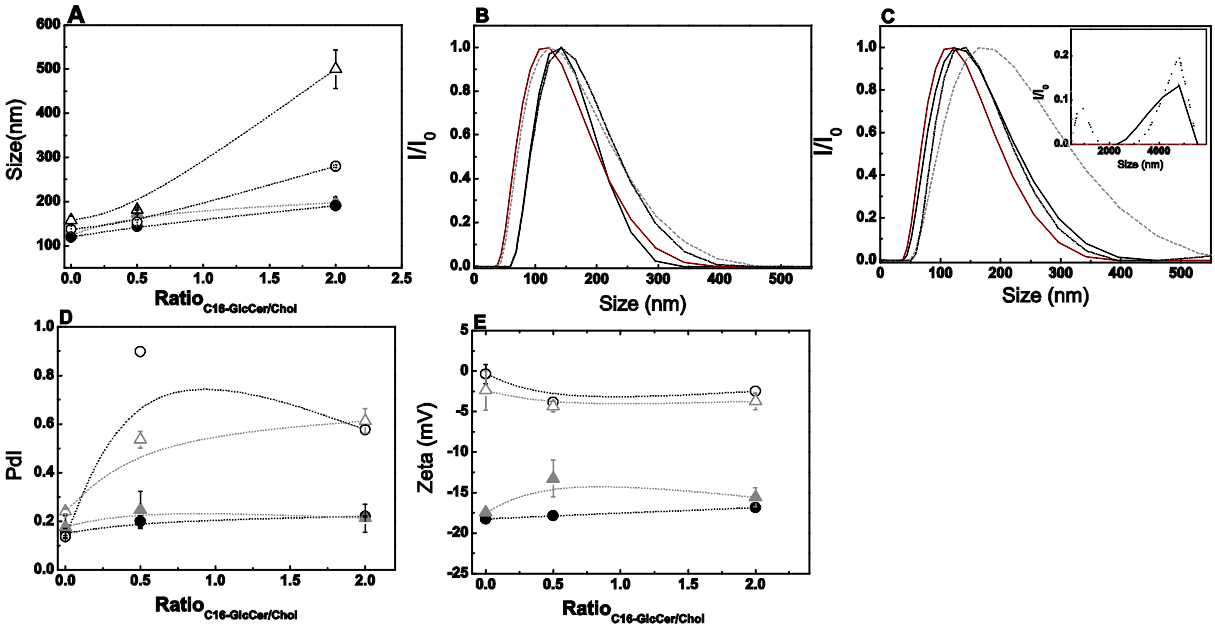

Figure S5. Characterization of POPC/Chol/C16-GlcCer mixtures by electrophoretic and dynamic light scattering measurements.

(A) Average size of POPC/Chol/GlcCer LUV containing 40 (triangles) and 70 (circles) mol% of POPC at pH 7.4 (solid symbols) and 5.5 (open symbols). (B, C) Normalized scattered light intensity of LUVs containing 40/40/20 (—), 40/20/40 (---), 70/20/10 (—), and 70/10/20 (-.-.-) of POPC/Chol/GlcCer, respectively, at (B) pH 7.4 and (C) pH 5.5. Inset shows vesicle population with sizes in the order of microns. (D) PdI and (E) ζ-potential of POPC/Chol/C16-GlcCer mixtures. Symbols are the same as in (A).

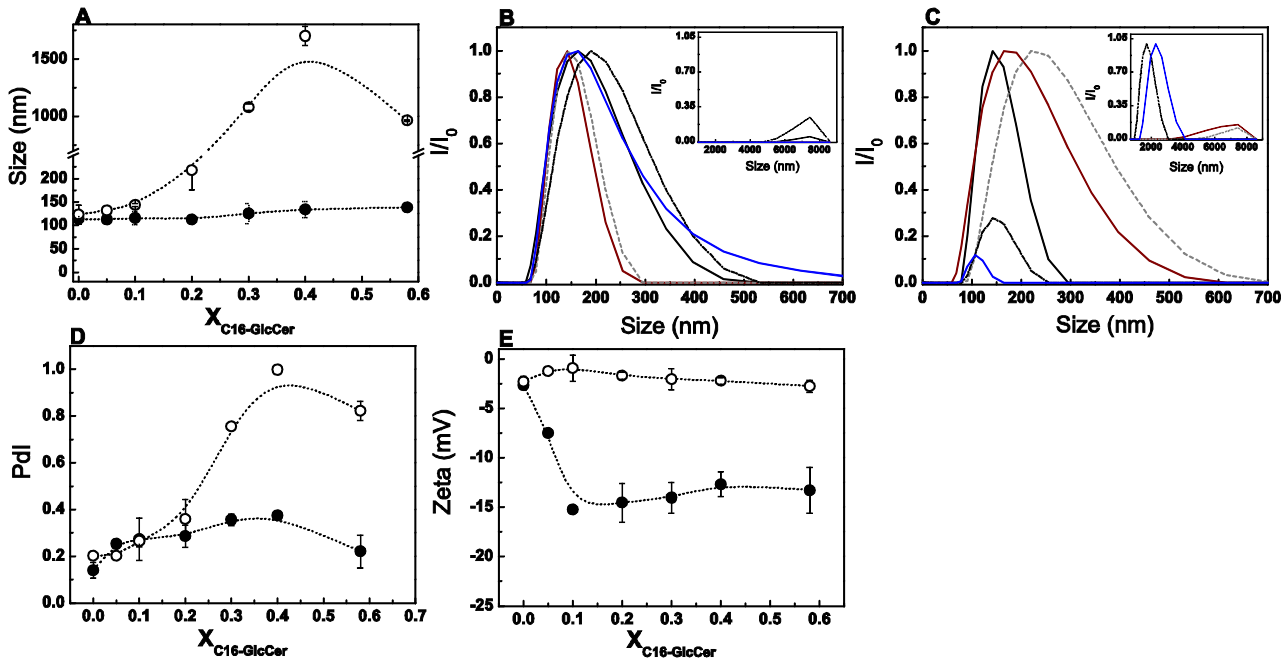

Figure S6. Characterization of POPC/C16-GlcCer binary mixtures by electrophoretic and dynamic light scattering measurements.

(A) Vesicle average size of POPC/C16-GlcCer LUVs at neutral (solid symbols) and acidic (open symbols) pH. (B, C) normalized scattered light intensity of LUVs composed by POPC 10 (—), 20 (—), 30 (---), 40 (-.-.-) and 58 (—) mol% of C16-GlcCer, at (B) pH 7.4 and (C) 5.5. Inset shows vesicle population with sizes in the order of microns. (D) PdI and (E) ζ-potential of POPC/C16-GlcCer LUVs at neutral (solid symbols) and acidic (open symbols) pH. Values are means ± SD of at least 3 independent experiments.

.

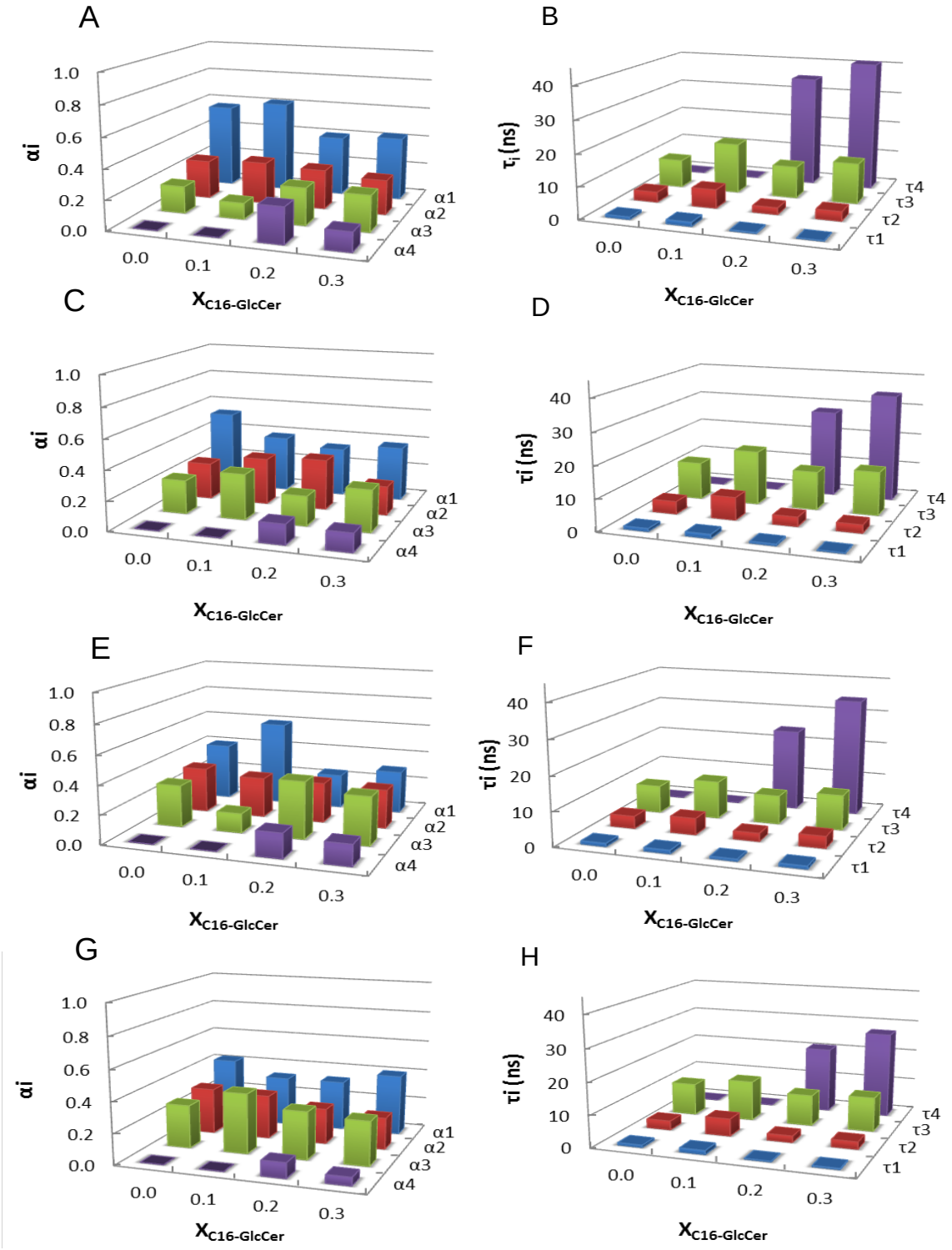

Figure S7. Analysis of t-PnA fluorescence intensity decay in POPC/Chol/C16-GlcCer mixtures with constant POPC/Chol ratio.

Variation of the pre-exponential factors and lifetime components of t-PnA fluorescence intensity decay, in POPC/Chol/C16-GlcCer ternary mixtures with a POPC/Chol ratio mimicking 25 (A, B, E, F) and 75 (C, D, G, H) mol % of $l_{o,}$ and increasing molar fractions of C16-GlcCer. Measurements were performed at (A-D) pH 7.4 and (E-H) pH 5.5. Values are means of at least 3 independent experiments.

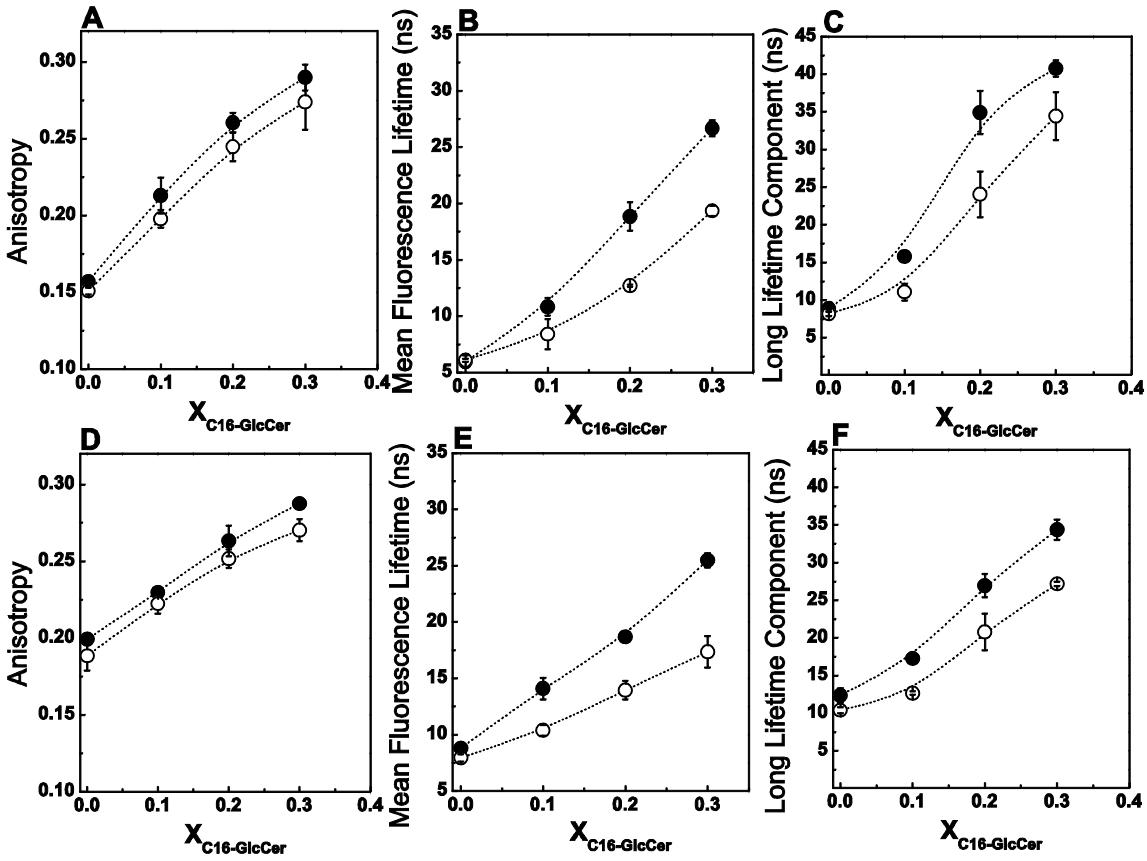

Figure S8. pH influence in the biophysical behavior of POPC/Chol/GlcCer membranes containing different l_o fractions.

t-PnA (A, D) fluorescence anisotropy, (B, E) mean fluorescence lifetime and (C, F) long lifetime component of the intensity decay in ternary POPC/Chol/C16-GlcCer mixtures containing POPC/Chol ratios mimicking (A-C) 25 and (D-F) 75 mol % of l_o phase. Measurements were performed at neutral (solid symbols) and acidic (open symbols) pH. Values are means ± SD of at least 3 independent experiments.

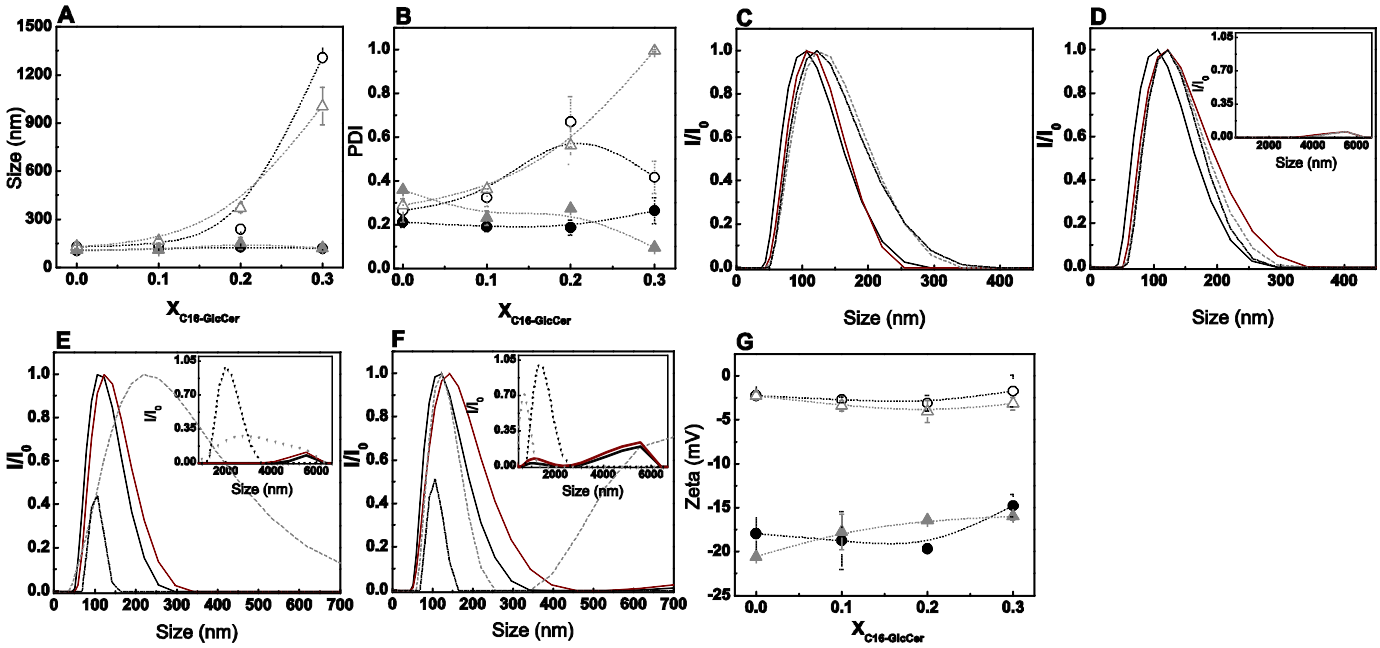

Figure S9. Characterization of POPC/Chol/C16-GlcCer LUVs containing constant POPC/Chol ratio by electrophoretic and dynamic light scattering measurements.

(A) Vesicle average size and (B) PdI of POPC/Chol/C16-GlcCer LUVs with POPC/Chol ratios mimicking 25 (circles) and 75 (triangles) mol % of $l_{o,}$ at neutral (solid symbols) and acidic (open symbols) pH. (C-F) Normalized scattered light intensity of LUVs containing a POPC/Chol ratio mimicking (C, E) 25 and (D, F) 75 mol % of l_o with 0 (—), 10 (—), 20 (---) and 30 (-.-.-) mol% of C16-GlcCer at (C,D) neutral or (E, F) acidic pH. Inset shows vesicle population with sizes in the order of microns. (G) ζ-potential of POPC/Chol/C16-GlcCer LUVs with POPC/Chol ratios mimicking 25 (circles) and 75 (triangles) mol % of $l_{o,}$ at neutral (solid symbols) and acidic (open symbols) pH. Values are means ± SD of at least 3 independent experiments.

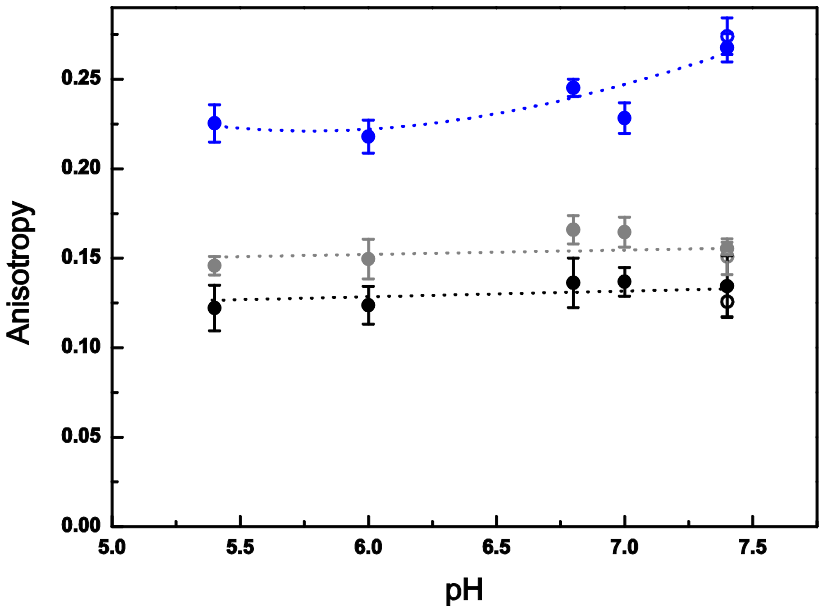

Figure S10. Influence of pH in the biophysical properties of POPC/C16-GlcCer lipid mixtures

Variation of t-PnA fluorescence anisotropy in mixtures containing POPC (black), and POPC with 5 (grey) and 30 (blue) mol % of GlcCer. The lipid mixtures are in citrate-phosphate buffers at different pH (solid circles) or in PBS (open circles). See supplementary Table 1 for more information on buffer composition. Values are means ± SD of at least 3 independent experiments.

Supplementary Tables

Table S1- Ions concentrations and ionic strength of the different buffers used in the study.

The ions concentration was calculated taking into account the concentration of the components of each buffer. The Ionic strength was directly determined in the buffers, using an osmometer.

pH	Total Cation concentration (M)		Total Anion concentration (M)	Ionic Strength (mOsm)
	Citrate-Phosphate buffer			
	Na^+	H^+	PO_4^{3-}	
5.40	0.22	0.11	0.11	286.00
6.00	0.25	0.13	0.13	283.00
6.80	0.31	0.15	0.15	326.00
7.00	0.33	0.16	0.16	333.00
7.40	0.36	0.18	0.18	350.00
	PBS buffer			
	Na^+	H^+	$PO_4^{3-} + Cl^-$	
7.40	0.17	0.01	0.16	291.00
	0.18			

Table S2. Molar fractions of POPC-rich, Chol-rich and GlcCer-rich phases (l_d, l_o and gel, respectively) in ternary POPC/Chol/C16-GlcCer mixtures.

The l_d, l_o and gel fractions were obtained from t-PnA mean fluorescence lifetime measurements (Fig. 3B, 3E, 5C and 5D), using the formalisms described in the Supplementary Information below.

			pH 7.4			pH 5.5		
$X_{C16\text{-}GlcCer}$			X_{ld}	X_{lo}	X_{gel}	X_{ld}	X_{lo}	X_{gel}
X_{lo}	0.25	0.1	0.58	0.42	0.00	0.54	0.46	0.00
		0.2	0.55	0.40	0.05	0.51	0.44	0.05
		0.3	0.47	0.34	0.20	0.44	0.39	0.17
	0.75	0.1	0.32	0.68	0.00	0.33	0.67	0.00
		0.2	0.30	0.67	0.04	0.31	0.65	0.04
		0.3	0.27	0.61	0.12	0.29	0.61	0.10
X_{POPC}	0.70	0.1	0.59	0.42	0.00	0.54	0.46	0.00
		0.2	0.69	0.22	0.08	0.66	0.24	0.10
	0.40	0.2	0.12	0.86	0.02	0.13	0.84	0.03
		0.4	0.40	0.29	0.30	0.47	0.41	0.13

Supplementary information

1. Determination of the fraction and composition of each phase for a three-phase situation of the POPC/Chol/C16-GlcCer ternary system

A. To calculate the fraction of each phase in POPC/Chol/C16-GlcCer mixtures we used a methodology previously developed by us (1):

First, the partition coefficient (K_p) of t-PnA towards a GlcCer-enriched gel phase and a Chol-enriched l_o phase was determined using t-PnA photophysical parameters obtained for the binary POPC/C16-GlcCer (2) and POPC/Chol mixtures (Fig. 1), respectively, accordingly to the following equations:

From mean fluorescent lifetime, $< \tau >$

$$< \tau > = (< \tau >_g K_p X_g + \overline{\tau}_f / \overline{\tau}_g < \tau >_f X_f) / K_p X_g + \overline{\tau}_f / \overline{\tau}_g X_f) \qquad \text{Eq. 1}$$

and from steady-state fluorescent anisotropy ,<r>

$$< r > = (< r >_g K_p X_g + \overline{\tau}_f / \overline{\tau}_g < r >_f X_f) / K_p X_g + \overline{\tau}_f / \overline{\tau}_g X_f \qquad \text{Eq. 2}$$

where X_i is the phase fraction, $< \tau >_i$, $\overline{\tau}_f$, and $<r>_i$, are the mean fluorescence lifetime, the lifetime weighted quantum yield and the steady-state fluorescence anisotropy of t-PnA, in phase *i*, respectively. K_p is obtained by fitting the equations to the data as a function of X_i.

B. The photophysical properties of t-PnA were used to calculate the fraction of light emitted from the C16-GlcCer-rich gel phase ($FL_{C16\text{-}GlcCer}$), as described in (1):

$$< \tau > = FL_{C16\text{-}GlcCer} <\tau>_{C16\text{-}GlcCer} + FL_{non\ C16\text{-}GlcCer} <\tau>_{nonC16\text{-}GlcCer} \qquad \text{Eq. 3}$$

where $<\tau>$ is the mean fluorescence lifetime obtained for these mixtures, $<\tau>_{C16\text{-}GlcCer}$ is the probe mean fluorescence lifetime in a C16-GlcCer-rich gel phase, $FL_{nonC16\text{-}GlcCer} = (1\text{-}FL_{C16\text{-}GlcCer})$ is the fraction of emitted light from all the C16-GlcCer poor phases, and $<\tau>_{nonC16\text{-}GlcCer}$ is the probe mean fluorescence lifetime in C16-GlcCer poor phases. In this ternary system the probe´s mean fluorescence lifetime in the C16-GlcCer poor phases is the value obtained in the absence of C16-GlcCer, and is given by:

$$< \tau >_{nonC16\text{-}GlcCer} = FL'_{Chol} <\tau>_{Chol} + FL'_{POPC} <\tau>_{POPC} \qquad \text{Eq. 4}$$

where FL'_i and $<\tau>_i$ are the fraction of light emitted and the probe´s mean fluorescence lifetime, respectively, in a Chol-rich l_o (*i* = Chol) and POPC-rich fluid phase (*i* = POPC) taken from the binary POPC/Chol mixtures. Using the fraction of light emitted from the Chol-rich and POPC-rich ($1\text{-}FL'_{Chol}$) phases (Eq. 4) and the total fraction of light emitted from the C16-GlcCer-poor phases (Eq. 3) it is then possible to calculate the fraction of light emitted from the Chol- and POPC- rich phases in ternary POPC/Chol/C16-GlcCer mixtures, FL_i using:

$$FL_i = FL'_i (1\text{-} FL_{C16\text{-}GlcCer}) \qquad \text{Eq. 5}$$

where *i* = Chol or POPC.

The K_p between two phases, α and β, $K_p^{\alpha/\beta}$ is given by:

$$K_p^{\frac{\alpha}{\beta}} = \frac{\chi_\alpha}{\chi_\beta} \frac{X_\alpha}{X_\beta} \quad \text{Eq. 6}$$

where χ_i is the fraction of probe in phase *i* = α or β, respectively.

The ratio of emitted light fraction from two phases, α and β, is given by:

$$FL_\alpha / FL_\beta = \frac{\chi_\alpha}{\chi_\beta} \frac{\overline{\tau_\alpha}}{\overline{\tau_\beta}} \quad \text{Eq. 7}$$

Assuming equal molar absorption coefficients in both phases, where FL_i is the fraction of emitted light from the phase *i*, χ_i, is the fraction of probe in phase *i*, and $\overline{\tau}_i$ is the probe lifetime-weighted quantum yield in phase *i* (*i* = α and β).
Solving equation 6 for the ratio of the probe fraction in each phase (χ_α / χ_β), and replacing in equation 7, the following equation is obtained:

$$FL_\alpha / FL_\beta = K_p^{\alpha/\beta} \frac{X_\alpha}{X_\beta} \frac{\overline{\tau_\alpha}}{\overline{\tau_\beta}} \quad \text{Eq. 8}$$

The molar fraction ratio of each phase, α and β, (X_α / X_β) is calculated from equation 8.
From the last equation the $X_{C16\text{-}GlcCer}/X_{POPC\ ratio}$ is calculated.
Knowing the $X_{C16\text{-}GlcCer}/X_{POPC}$ and X_{Chol}/X_{POPC} for the mixtures under study, the POPC-rich phase fraction is obtained, since $X_{C16\text{-}GlcCer} + X_{Chol} + X_{POPC} = 1$.

2. Determination of the tie-triangle boundaries

Taking into account the phase fractions of the experimental samples, the pure l_o phase (taken from the POPC/Chol binary phase diagram (3)) and pure gel phase (taken from the POPC/GlcCer binary phase diagram (2)), it was possible to calculate the boundaries of the tie-triangle using our previous established iterative method (1). To estimate the boundaries of the tie-triangle, the phase fraction of each mixture were used (see Table 2) and the lever rule, which is valid inside the tie-triangle, was applied based on the following considerations: inside the tie-triangle the composition of each phase can be calculated by drawing a straight line from each corner of the tie-triangle through each experimental point to its intersection with the opposite side (i.e., to calculate the X_{ld} of point *a*, a line is drawn from point *F* through point *a* to its intersection with the opposite side, *a'*, the X_{ld} is calculated by the ratio between the distances $\overline{aa'}$ and $\overline{Fa'}$ (see Figure S8)).

3. Determination of the l_o/l_d phase boundaries

The limits of l_o/l_d phase coexistence were determined taking into account POPC/Chol and POPC/C16-GlcCer binary systems and also the experimental points that corresponded to mixtures displaying l_o/l_d phase coexistence. The lever-rule is also applied to this region of the phase diagram, and the the l_o+l_d boundaries can be calculated, using the determined tie-lines. To calculate the length and direction of the tie-lines, several thermodynamic considerations were taken into account: *i*) the tie-lines must connect the upper and lower boundary of l_o+l_d phase and simultaneously pass through the experimental points; *ii*) the ratio between the distance of the lower boundary to a specific composition and the total length of the tie line should correspond to the l_o fraction of the sample; *iii*) due to thermodynamic restrictions tie lines should never cross and should present a fanwise trend between the lateral boundaries of the phase in question (see Fig S8, black lines in the l_o+l_d phase) (4). Fig. S11 shows two possible tie-lines in the l_o+l_d phase. Quantitative determination of the phase fraction of the studied mixtures using these two tie-lines retrieves similar values, suggesting that these tie-lines correspond to the uncertainty associated to our method.

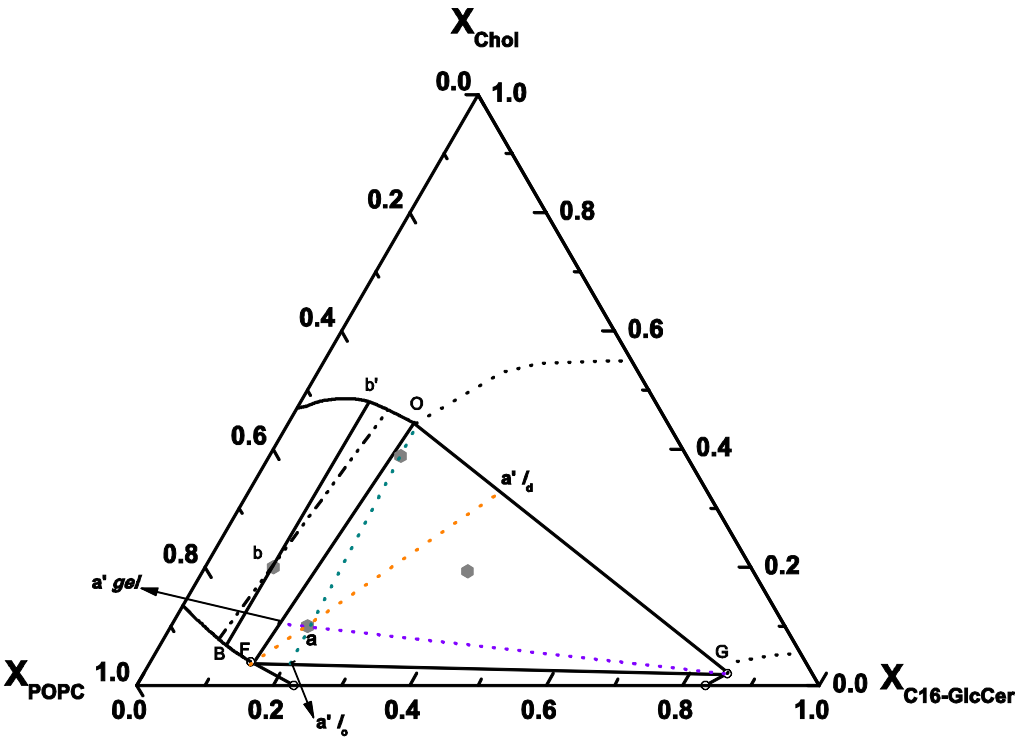

Figure S11. Determination of the phase fractions and phase boundaries of POPC/Chol/C16-GlcCer ternary phase diagram.

POPC/Chol/C16-GlcCer ternary phase diagram (pH 5.5). The tie-lines (black lines) in the l_o+l_d phase, allowed the determination of the upper boundary of the l_o+l_d phase. Determination of the phase fractions inside the tie-triangle were performed as described in the

supporting text. The three lines exemplify the method used for the determination of the l_d (orange), l_o (green) and gel (purple) phase fraction of the ternary mixture *a*.

Supporting References

1. Castro, B. M., R. F. M. Almeida, L. C. Silva, A. Fedorov, and M. Prieto. 2007. Formation of Ceramide/Sphingomyelin Gel Domains in the Presence of an Unsaturated Phospholipid: A Quantitative Multiprobe Approach. Biophys J 93:1639-1650.
2. Varela, A. R. P., A. M. P. S. Gonçalves da Silva, A. Fedorov, A. H. Futerman, M. Prieto, and L. C. Silva. 2013. Effect of glucosylceramide on the biophysical properties of fluid membranes. Biochim Biophys Acta 1828:1122-1130.
3. de Almeida, R. F. M., A. Fedorov, and M. Prieto. 2003. Sphingomyelin/Phosphatidylcholine/Cholesterol Phase Diagram: Boundaries and Composition of Lipid Rafts. Biophys J 85:2406-2416.
4. Rhines, F. N. 1956. Phase diagrams in metallurgy: their development and application. McGraw-Hill.